Some Studies Verify the Applicability of the Free Vibration Method of Crack Detection in Composite Beams for Different Crack Geometries

Vikas KHALKAR
Faculty, Department of Mechanical Engineering, Gharda Institute of Technology, Lavel, India, vikas_khalkar@rediffmail.com

Pon HARIHARASAKTHISUDHAN
Faculty, Department of Mechanical Engineering, Sri Krishna College of Technology, Kovaipudur, Coimbatore, Tamil Nadu, India, harimeed2012@gmail.com

Kamaraj LOGESH
Faculty, Department of Mechanical Engineering, Vel Tech Rangarajan Dr. Sagunthala R&D Institute of Science and Technology, Chennai, India, klogesh7@gmail.com

Arul MOSHI
Faculty, Department of Mechanical Engineering, National Engineering College, Kovilpatti, India, moshibeo2010@gmail.com

Jyoti BORADE
Faculty, Department of Computer Engineering, Gharda Institute of Technology, Lavel, India, jvkhalkar@git-india.edu.in

Rohan KALAMKAR
Faculty, Department of Mechanical Engineering, Gharda Institute of Technology, Lavel, India, rrkalamkar@git-india.edu.in

Abstract: - Defect detection and classification are important issues as they cause structures to catastrophic failure. Many flaws have already been addressed, but non-destructive testing techniques for composite materials have been widely used. However, the impact of arbitrary and unpredictable flaw geometry on these approaches' applicability has yet to be observed. This paper considers the cases of a previously published article, i.e., pultrusion-produced orthotropic (GFRP) cracked cantilever beam, to determine the crack location and depth. In contrast to the well-known V-shaped crack, a new fracture model (a combination of rectangular and V-shaped) is presented due to its practical importance. Using ANSYS software, FEA simulations were carried out on the new and V-shaped crack models for the natural frequencies. The maximum percentage error for the natural frequency between new and V-shaped crack models for the same configurations was only up to 1.815. Then, the ANN model was trained using the natural frequencies dataset of V-shaped cracked cases only. Afterward, the ANN model was used for predicting the crack locations and crack depths in beams, i.e., V-shaped cracked beams and a combination of rectangular and V-shaped (new crack model) cracked beams. The ANN model gave good results for predicting the crack locations and depths in composite cantilever beams irrespective of the crack geometries. Hence, it is clear that even though the ANN model was trained using the dataset of V-shaped cracked cases, it accurately predicts the crack locations and depth in the beams, which have had new geometry.

Keywords: - ANN, Hidden layer, Natural frequency, FEA, Crack depth, and Crack location.

1. INTRODUCTION

In the civil, automotive, and aerospace industries, composites are used in various structural applications. Beams are a typical example of how composites are used in structures. A composite beam can be destroyed by cracks that grow over time. The focus of recent research is the identification or diagnosis of the emergence of faults in composites under free vibration loading. A new technique for numerically simulating the free vibration of a cantilever composite beam with several open, non-propagating cracks was presented by Kisa [1]. The author noticed that the frequency ratios decreased when the fiber angle increased. Krawczuk et al. [2] discovered that the crack in a structural composite member beam affected the beam's natural frequencies: the rise in crack depth had resulted in a drop in the calculated natural bending frequencies. On the other hand, Song et al. [3] examined how many surfaces crack affected a cantilever laminated composite beam's ability to bend freely. Transverse shear and inertia effects were considered in the governing equations of the composite beam with open fractures. Finally, a composite beam with various fiber orientations and a single crack was studied by Hamid and Hamada [4]. They claimed that for a constant crack location and depth, the natural frequency and the damping ratio increased as the fiber angle grew. A fiber-reinforced composite cantilever with an edge surface crack was explored by Wang et al. [5] for its combined bending and torsional vibration. They concluded that fiber orientation and volume fraction affected these variations in natural frequencies and the accompanying mode shapes. Aye and Htike [6] used the first two relative natural frequencies to predict the crack parameters in the cantilever beam. They tested the cracked cantilever beams for the first two natural frequencies. Afterward, they developed a correlation model to identify the locations and depths of the crack in cantilever beams. Sadettin et al. [7] studied the effect of crack geometry on the natural frequency of composite beams. They considered a V-shaped crack with the new crack model (combination of V-shape and rectangular-shaped crack). The research study found that natural frequencies decrease as crack depth increases. Modal frequencies and mode shapes have reduced as a result of these modifications. Hence by evaluating changes in the vibration parameters [8], crack characteristics can be predicted. A model of a damaged structure and genetic algorithms (GAs) based crack diagnosis method is proposed. An analytical model of a cracked cantilever beam was used to simulate the cracked-beam structure, and natural frequencies were calculated using numerical techniques. This approach used genetic algorithms to keep track of any changes in the structure's natural frequencies. When the crack location and depth in the cantilever beam are identified as an optimization problem, binary and continuous genetic algorithms (BGA and CGA) are used to minimize the cost function based on the difference between measured and calculated natural frequencies in order to find the optimal location and depth in the cantilever beam. Khatir et al. provide [9] a technique for quantification, localization, and non-destructive detection of different defects in simple and continuous beams and a more complex structure, the two-dimensional frame structure. The proposed technique uses the Firefly Algorithm and Genetic Algorithm as optimization methods, while the Coordinate Modal Assurance Criterion is used as an objective function. The results imply that using the suggested combination of the Coordinate Modal Assurance Criterion with the Firefly Algorithm or Genetic Algorithm to detect different local structural faults in complex constructions quickly might be beneficial. In most circumstances, visual examination of cracks and damages is ineffective and unnecessary; hence, non-destructive testing (NDT) techniques like thermography, ultrasonic testing, and X-ray diffraction are used to forecast damage in structures. These solutions, however, need time and money. As a result, additional potential techniques are being developed.

The employment of mathematical methodologies, vibration-based methods [10], and soft-computing techniques like artificial neural networks (a branch of artificial intelligence) are promising and desirable in this context. Nasiri et al. provided [11] a review study on mechanical fault detection using Artificial Intelligence (AI) approaches. They spoke about Bayesian networks, genetic algorithms (GA), fuzzy logic, case-based reasoning, and artificial neural networks (ANN). Sutar et al. proposed a neural network-based controller to study transverse cracks in cantilever beams. Teidj et al.5 utilized [12] the crack stiffness to beam elemental stiffness matrix to generate a homogeneous linear elastic beam finite element. They detected crack defect features by measuring changes in beam frequencies and observing their fluctuations. Thatoi et al. described [13] the Cascade Forward Back Propagation (CFBP) network, which uses changes in natural frequencies and measurements to identify cracks in structural beams. To detect crack characteristics, Pan et al. proposed [14] a two-stage strategy combining an artificial neural network (ANN) and a genetic algorithm (GA). In order to examine the influence of geometry modification on natural frequencies and mode shapes under free vibration loading.

Gillich et al. [18] proposed two machine learning methods, random forest (RF) and the artificial neural network (ANN), as searching tools in this paper. Their databases contain damage scenarios for a prismatic cantilever beam with one crack and ideal and non-ideal boundary conditions. The crack assessment was made in two steps. First, a coarse damage location was found from the networks trained for scenarios comprising the whole beam. Afterward, the assessment was made involving a particular network trained for the segment of the beam on which the crack was previously found. They used the two machine learning methods to estimate the crack location and severity with high accuracy for both simulation and laboratory experiments. Regarding the location of the crack, which was the main goal of the practitioners, the errors were less than 0.6%. Based on these achievements, they concluded that the damage assessment we proposed, in conjunction with the machine learning methods, is robust and reliable. In this paper, Tufisi et al. [19] proposed a model for detecting transverse cracks in simply supported beams, which can be part of more complex structural systems. The relative frequency shifts of the structure are considered a basis for damage identification. An original method developed by the authors is employed to evaluate the required modal parameters. A multi-stage optimization approach based on the rigidity loss suffered by the affected structure is employed to recognize the locations of potential cracks accurately. The outcome presented in this research shows the computational ability of the proposed model to indicate the presence and location of damages in the beam-like structures. In this study, Tufisi et al. [20] present a method (DS-SHC) used for estimating the DS for closed and open transverse cracks in beam-like structures using the intact and damaged beam deflections under its weight and a Stochastic Hill Climbing (SHC) algorithm. After describing the procedure of applying DS-SHC, we calculate for a prismatic cantilever beam the severities for different crack types and depths. The results are tested by comparing the DS obtained with DS-SHC with those acquired from dynamic tests made using professional simulation software. We obtained a good fit between the severities determined in these two ways. Subsequently, they performed laboratory experiments and found that the severities obtained with the DS-SHC method can accurately predict the frequency changes due to the crack. Hence, these severities are a valuable tool for damage detection. In this paper, Tufisi et al. [21] proposed an analytical approach for generating the data needed to train a Random Forest model (RF) that will perform the SHM task to detect, locate, and assess the severity of transverse cracks in beam-like structures. Using an original method, they calculated the relative frequency shifts (RFS) for different damage scenarios and used the generated data to train the RF model. The results indicate that the RF model can detect the presence of the defect and find the position and depth of the transverse cracks very precisely if the crack is located in the area where the beam achieves the maximum bending moment. By correctly categorizing accelerometer data, deep learning algorithms achieve the objective [22] of evaluating the condition of beams in a non-invasive manner. While an essential indicator, the high probabilistic accuracy attained on the validation set is typically insufficient in most practical circumstances. When damage occurs, the accurate prognosis must also be comprehensible to humans, considering the factors that led to that specific outcome. It will increase confidence and the chance of rectifying functioning conditions in the future.

In previous research studies, V-shaped crack geometry was considered in the beams. However, cracks created in beams in [7] real life have a rectangular upper side and a V-shape towards the crack tip. Therefore, this research study introduces a new crack model with the known V-shaped crack model to investigate the effect of crack geometry change on the natural frequency under free vibration loading. These examinations were carried out using finite element analysis. The data set of the first three normalized natural frequencies V-shaped cracked cases was used to train the machine learning model. Afterwards, the train ANN model was used to predict the crack parameters for different crack geometries. The machine learning model accurately predicted the crack location and depth in the cantilever beam irrespective of the crack geometry.

2. MATERIAL AND GEOMETRIC PROPERTIES OF THE BEAM

The material properties of the GFRP composite [7] beams are given in Table 1. The beam had a solid cross-section of 29 mm width, 45 mm thickness and an effective length of 1300 mm.

Table 1 Material properties of GFRP composite beam [7]

E_1 *(N/m²)*	25e9
E_2 *(N/m²)*	8.5e9
E_3 *(N/m²)*	8.5e9
G_{12} *(N/m²)*	3e9
G_{13} *(N/m²)*	3e9
G_{23} *(N/m²)*	3.9e9
μ_{12}	0.23
μ_{13}	0.23
μ_{23}	0.09
Þ *(kg/m³)*	1800

3. SIMULATED CRACK CONFIGURATIONS

In this study, one intact specimen and 142 cracked specimens of GFRP materials were considered to investigate the effect of different cracks on the natural frequencies of a cantilever beam. Two crack parameters, i.e., crack location ratio, and crack depth ratio, were considered. The ratio between the distance of the crack from the cantilevered end and the length of the beam was considered as the crack location ratio (L_1/L). Similarly, the ratio between the depth of the crack and the depth of the beam was considered as the crack depth ratio (a/H). Furthermore, two separate cases were considered, i.e., case 1 and case 2.

Case 1: One hundred twenty-five specimens of V-shaped cracked cases were considered in this case. This case was subdivided into five sub-cases. In the first sub-case, 25 specimens were considered. A 145 mm location was chosen for the crack from the cantilevered end, and at this location, on the first specimen, the crack depth ratio (a/H) was chosen as 0.1; furthermore, on the subsequent 24 specimens, the crack depth ratio was varied from 0.11111 to 0.666667 by an interval of 1mm. The second, third, fourth, and fifth sub-cases were similar to that of the first sub-case; the only difference was that instead of 145 mm crack location; 345, 545 mm, 745 mm, and 945 mm cracks locations were chosen for the second, third, fourth and fifth sub-cases respectively.

Case 2: In this case, 17 specimens of the new crack model were considered. Out of 17, 10 specimens were used to test the machine learning model based on the V-shaped cracked cantilever beam data. Furthermore, seven specimens were used to find the numerical natural frequencies and validate the experimental results. The schematic representation of a cracked cantilever beam is shown in Figure 1. The one case of the V-shaped and new crack model (combination of rectangular and V-shaped) are shown in Figures 2 and 3, respectively.

4. FINITE ELEMENT MODELING AND ANALYSIS

ANSYS [15] finite element program was used to determine the natural frequency of cracked cantilevered beams. For this purpose, a rectangular zone of the required geometric properties was created, and then this zone was extruded to obtain the model in three dimensions. A small area of dimensional requirements was created and extruded to represent the crack in the primary model. After that subtract command was used for subtracting the small volume from the volume of the primary model. Then a cracked three-dimensional model gets obtained. For finite element modeling of a cracked beam, solid 95, solid 185, and solid 186 elements were used. Results of natural frequencies remained [16–17] almost the same irrespective of the elements used in the analysis. Hence, for all the simulations, a 20-node structural solid element (solid 186) was chosen for modeling the beam. This element has some unique features, i.e., stress stiffening, considerable strain, and large deflection. Finite element boundary conditions were applied on the beam to constrain all degrees of freedom of the cantilevered end of the beam.

The Block Lanczos eigenvalue solver was used to compute the natural frequencies of cracked beams. The mesh-independent study was carried out to check the reliability of the FEA model on the cracked beams. Through a mesh-independent study, it was found that natural frequency results were independent of the mesh size. Figure 4 and 5 illustrate a few bending modes shapes plots.

5. ARTIFICIAL NEURAL NETWORK MODELING AND ANALYSIS

ANN technique is used for crack prediction in beams. The ability to learn from experience in order to enhance results is the most important aspect of ANN. As a consequence, ANN can be used in a number of applications, including classification, control systems, detection, image processing, and pattern recognition. The artificial Neural Network classifier is based on the human brain structure. Nodes are connected with the neurons in the brain. It is a feed-forward artificial neural network where the mapping between inputs and output is nonlinear. It has input and output layers and multiple hidden layers with many neurons.

The learning methodology adopted to train an ANN is Back propagation. The learning process combines many hidden layers, the number of nodes in each of the hidden layers, and connection weight. Backpropagation allows for the adjustment of the weights in the network iteratively. Inputs were combined with the initial weights and fed to the nonlinear activation function. From the hidden layers to the output layer, each layer's output is fed as input to the next layer. Output is compared with the expected value. The computed errors are propagated backward from the output to the preceding layer. The error propagated back to adjust the interconnection weights between the layers. Back propagation is done using a Gradient Descent. The partial derivative of the Mean Squared Error function was calculated for interconnection weights. Then, to propagate the error back, the weights of the first hidden layer were updated with the gradient value. This process kept going until the gradient for each input-output pair converged. The general architecture of ANN is shown in Figure 6.

The ANN model was used to train the normalized bending natural frequencies data, which is listed in Table 3A, Table 3B and Table 3C. This data was prepared using the data of V-shaped cracked cases. Table 4 and 5 present the testing data. 93.33% of the data and 6.66% of data were used to train and test the neural network model. The ANN model was implemented with three input layers, nine hidden layers, and two output layers.

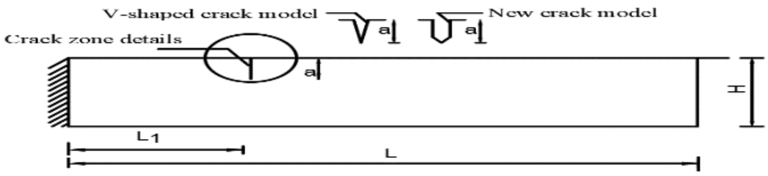

Figure 1. A schematic representation of a cracked cantilever beam

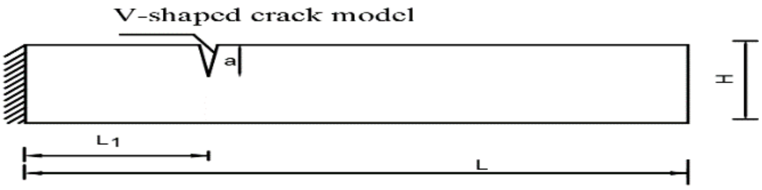

Figure 2. Cracked cantilever beam with V-shaped crack

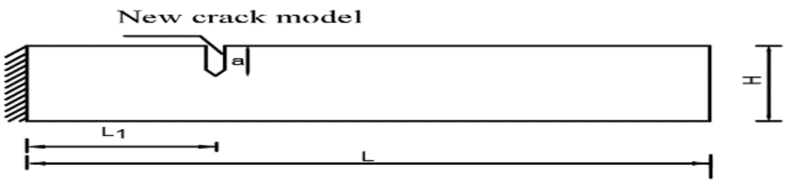

Figure 3. Cracked cantilever beam with a combination of rectangular and V-shaped cracks (new crack model)

Figure 4. First bending mode shapes of a cracked cantilever beam with a V-shaped crack, crack location 745 mm, crack depth 25 mm

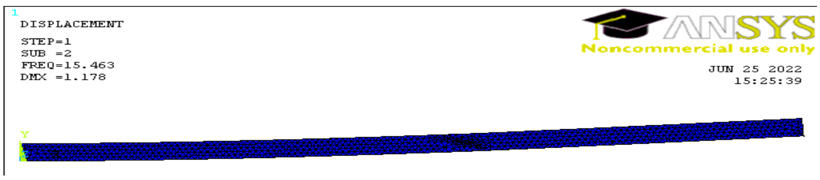

Figure 5. First bending mode shapes of a cracked cantilever beam with a combination of rectangular and V-shaped crack (new crack model), crack location 745 mm, crack depth 25 mm

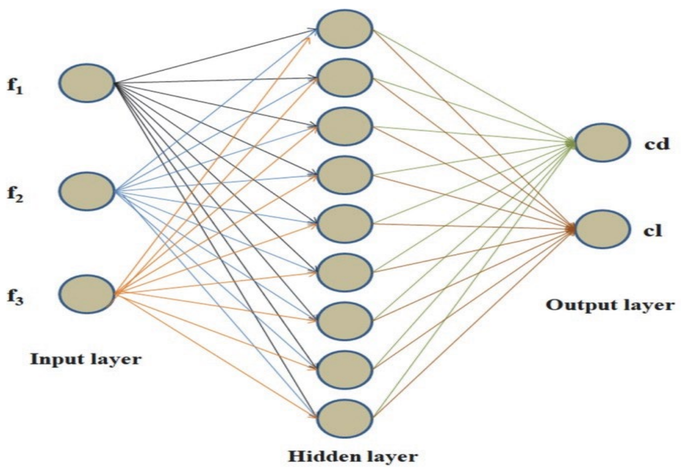

Figure 6. Architecture of ANN

First, three normalized bending natural frequencies were chosen as input parameters; relative crack location and depth were selected as output parameters. ANN maps these inputs with the outputs. Using the hyper-parameters, the ANN model was tuned. The hyper-parameters are listed in Table 2. Artificial neural networking (ANN) in MATLAB is used to analyse and predict the depth and position of crack in the beam and data obtained by training is validated by the analytical results. In MATLAB, the desired inputs and outputs or targets are imported in the workspace and using "nntool" network is created using inputs and targets. Figure 6 shows the architecture of a neural network. Here, a typical three-layered Feed Forward Back Propagation (FFBP) neural network is considered consisting of three neurons in input layer, nine neurons in hidden layer and two neurons in output layer as shown in Figure 7. The first three relative natural frequencies (f_1, f_2, and f_3) are taken as input parameters; crack location and crack depth were taken as output parameters. The various functions used are: Levenberg Marquardt (trainlm) is taken as Training function, LEARNGDM is taken as adaption learning function, Mean square error (MSE) taken as performance function and Sigmoid function (tansig) as transfer function. The regression plot regarding training, validation and testing are shown in Figure 8. It shows that the predicted data are well fitted to the actual output.

Table 2 Hyper-parameter of Artificial Neural Network

Sr. No.	*Input parameters for training*	*Values*
01	Learning rate	0.1
02	Number of epochs	1000
03	Number of nodes in input layer	03
04	Number of neurons in the hidden layer	09
06	Number of nodes in output layer	02
07	Goal	zero

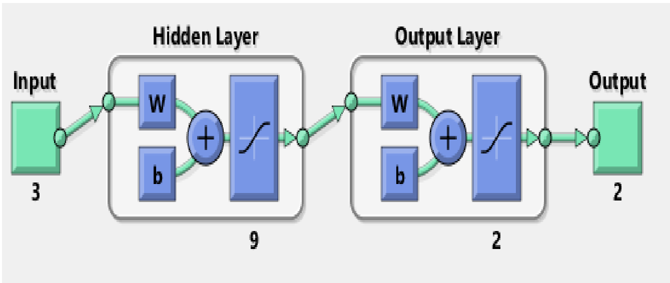

Figure 7. Feed forward back propagation network

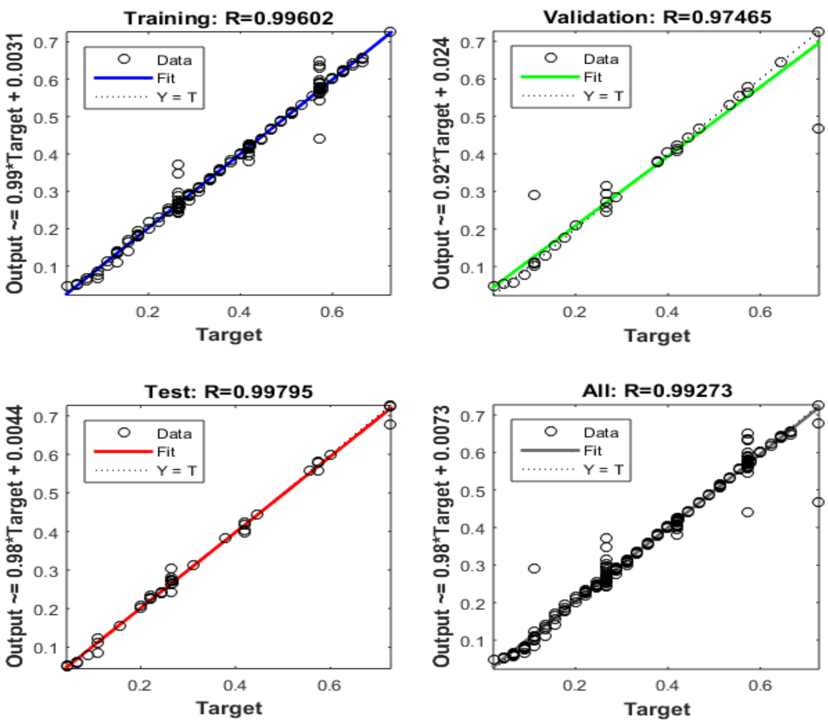

Figure 8. Regression analysis plot

Table 3A Training data of V-shaped cracked cases to the neural network for two crack locations ratio, i.e., $L_1/L = 0.1115$ and $L_1/L = 0.2654$

Sr. No.	*a/H*	*For crack location $L_1/L = 0.1115$*			*For crack location $L_1/L = 0.2654$*		
		f_{r1}	f_{r2}	f_{r3}	f_{r1}	f_{r2}	f_{r3}
1	0.1	0.993997	0.998224	0.9998888	0.996623	0.999686	0.997003
2	0.111111	0.992497	0.9978	0.999852	0.995748	0.999605	0.996226
3	0.133333	0.988745	0.996739	0.999778	0.993685	0.999413	0.994413
4	0.155556	0.984431	0.995514	0.999667	0.991246	0.99918	0.992341
5	0.177778	0.979085	0.994016	0.999575	0.988245	0.998896	0.989714
6	0.2	0.973739	0.992517	0.999482	0.984493	0.998542	0.986532
7	0.222222	0.96636	0.990472	0.999297	0.980742	0.998187	0.983351
8	0.244444	0.958857	0.988441	0.999131	0.976271	0.997767	0.979651
9	0.266667	0.951354	0.986411	0.998964	0.9718	0.997347	0.975951
10	0.288889	0.94185	0.98392	0.998761	0.965735	0.996775	0.971067
11	0.311111	0.932345	0.981429	0.998557	0.95967	0.996203	0.966183
12	0.333333	0.921528	0.97868	0.998317	0.953104	0.995585	0.96104
13	0.355556	0.910711	0.975931	0.998076	0.946539	0.994967	0.955898
14	0.377778	0.898518	0.972979	0.997817	0.938942	0.994264	0.9502
15	0.444444	0.857688	0.963436	0.996966	0.931345	0.99356	0.944502
16	0.466667	0.840618	0.959724	0.996615	0.921403	0.992654	0.937361
17	0.488889	0.823548	0.956013	0.996263	0.911461	0.991747	0.930221
18	0.511111	0.804258	0.952079	0.995838	0.874633	0.988431	0.905727
19	0.533333	0.784968	0.948145	0.995412	0.860314	0.98716	0.896589
20	0.555556	0.763584	0.944105	0.995005	0.845057	0.985829	0.887524
21	0.577778	0.7422	0.940065	0.994598	0.829801	0.984497	0.878459
22	0.6	0.719784	0.936167	0.994136	0.80926	0.982781	0.867341
23	0.622222	0.697368	0.932268	0.993673	0.78872	0.981065	0.856223
24	0.644444	0.670356	0.928035	0.993174	0.766523	0.979257	0.845401
25	0.666667	0.643344	0.923803	0.992674	0.744326	0.97745	0.834579

Table 3B Training data of V-shaped cracked cases to the neural network for two crack locations ratio, i.e., $L_1/L = 0.4192$ and $L_1/L = 0.5731$

Sr. No.	*a/H*	*For crack location $L_1/L = 0.4192$*			*For crack location $L_1/L = 0.5731$*		
		f_{r1}	f_{r2}	f_{r3}	f_{r1}	f_{r2}	f_{r3}
1	0.1	0.1	0.998405	0.996778	0.999468	0.995929	0.998575
2	0.111111	0.111111	0.998062	0.996061	0.999312	0.994947	0.998224
3	0.133333	0.133333	0.996874	0.993692	0.999	0.992375	0.997336
4	0.155556	0.155556	0.995936	0.991839	0.998624	0.989611	0.996411
5	0.177778	0.177778	0.994435	0.988902	0.998124	0.9863	0.995264
6	0.2	0.2	0.992653	0.9855	0.997436	0.981475	0.993501
7	0.222222	0.222222	0.990871	0.982097	0.996749	0.97665	0.992008
8	0.244444	0.244444	0.98862	0.977855	0.995998	0.971556	0.990147
9	0.266667	0.266667	0.986369	0.973612	0.995248	0.966463	0.988604
10	0.288889	0.288889	0.983493	0.968458	0.994341	0.960661	0.986484
11	0.311111	0.311111	0.980617	0.963304	0.993435	0.954859	0.984794
12	0.333333	0.333333	0.977146	0.957228	0.992059	0.946237	0.981643
13	0.355556	0.355556	0.973676	0.951153	0.990683	0.937615	0.979355
14	0.377778	0.377778	0.969424	0.94411	0.989152	0.928724	0.976106
15	0.444444	0.4	0.965172	0.937068	0.98762	0.919834	0.973842
16	0.466667	0.422222	0.96067	0.92997	0.985712	0.909409	0.970033
17	0.488889	0.444444	0.956168	0.922871	0.983805	0.898984	0.967589
18	0.511111	0.466667	0.949447	0.912963	0.981273	0.886114	0.962887
19	0.533333	0.488889	0.942725	0.903055	0.978741	0.873244	0.960152
20	0.555556	0.511111	0.934346	0.891679	0.975489	0.858481	0.954758
21	0.577778	0.577778	0.907334	0.857337	0.972238	0.843717	0.95205
22	0.6	0.6	0.894766	0.843449	0.968142	0.82701	0.945945
23	0.622222	0.622222	0.882198	0.829561	0.964047	0.810302	0.943355
24	0.644444	0.644444	0.867348	0.815238	0.946883	0.753531	0.926952
25	0.666667	0.666667	0.852498	0.800915	0.940099	0.733244	0.92493

Table 3C Training data of V-shaped cracked cases to the neural network for location ratio, i.e., $L_1/L = 0.7269$

Sr. No.	***a/H***	***For crack location $L_1/L = 0.7269$***		
		f_{r1}	f_{r2}	f_{r3}
1	0.1	0.999921	0.998076	0.995208
2	0.111111	0.999906	0.9976	0.994043
3	0.133333	0.999875	0.996648	0.991712
4	0.155556	0.999781	0.995231	0.98829
5	0.177778	0.999687	0.993813	0.984868
6	0.2	0.999562	0.991763	0.980039
7	0.222222	0.999437	0.989712	0.975211
8	0.244444	0.999281	0.98715	0.969439
9	0.266667	0.999125	0.984588	0.963667
10	0.288889	0.998937	0.981576	0.957174
11	0.311111	0.998749	0.978564	0.950681
12	0.333333	0.998499	0.974326	0.942042
13	0.355556	0.998249	0.970088	0.933402
14	0.377778	0.997937	0.965127	0.924005
15	0.444444	0.997624	0.960165	0.914607
16	0.466667	0.99728	0.954793	0.905209
17	0.488889	0.996936	0.949421	0.895812
18	0.511111	0.996373	0.941275	0.882899
19	0.533333	0.995811	0.933129	0.869987
20	0.555556	0.995154	0.923504	0.856556
21	0.577778	0.994498	0.91388	0.843126
22	0.6	0.993685	0.90304	0.829973
23	0.622222	0.992872	0.8922	0.81682
24	0.644444	0.991653	0.87653	0.800799
25	0.666667	0.990433	0.86086	0.784779

Table 4 Testing data of V-shaped cracked cases to the neural network

Sr.no.	***L_1/L***	***a/H***	***V-shaped cracked cases: Relative natural frequency***		
			f_{r1}	f_{r2}	f_{r3}
01	0.1115	0.4	0.886325	0.970027	0.997558
02	0.1115	0.422222	0.872007	0.966731	0.997262
03	0.2654	0.466667	0.900206	0.990725	0.922543
04	0.2654	0.488889	0.888951	0.989702	0.914866
05	0.4192	0.533333	0.925968	0.880302	0.961410
06	0.4192	0.555556	0.916651	0.868819	0.958007
07	0.5731	0.6	0.958857	0.792060	0.936690
08	0.5731	0.622222	0.953667	0.773819	0.934364
09	0.7269	0.644444	0.988901	0.843272	0.778045
10	0.7269	0.666667	0.987369	0.825683	0.771311

Table 5 Testing data of new cracked model cases (combination of rectangular and V-shaped)

Sr.no.	***L_1/L***	***a/H***	***V-shaped cracked cases: Relative natural frequency***		
			f_{r1}	f_{r2}	f_{r3}
01	0.1115	0.4	0.8863224	0.9700274	0.9975510
02	0.1115	0.422222	0.8720010	0.9667310	0.9972610
03	0.2654	0.466667	0.9002016	0.9907220	0.9225400
04	0.2654	0.488889	0.8889410	0.9897003	0.9148601
05	0.4192	0.533333	0.9259616	0.8803015	0.9614028
06	0.4192	0.555556	0.9166414	0.8688120	0.9580036
07	0.5731	0.6	0.9588510	0.7920580	0.9366822
08	0.5731	0.622222	0.9536582	0.7738186	0.9343612
09	0.7269	0.644444	0.9889000	0.8432718	0.7780433
10	0.7269	0.666667	0.9873622	0.8256810	0.7713104

6. RESULTS AND DISCUSSIONS

The free vibrations of intact and cracked beams with different crack depths are studied using the finite element analysis. Determining the beams' natural frequencies and investigating the connection between crack depth and natural frequency fluctuation. The first two natural frequencies are displayed in Table 6. Natural frequencies, such as V-shaped fracture cases and innovative crack models (combination of rectangular and v-shaped), were estimated for the intact and cracked beams. First, it has been observed that the natural frequencies drop as the beams' crack depth rises. From Figure 9 the maximum difference of 1.815 percent was found when comparing the finite element natural frequency from the new and V-shaped crack models for the same configurations.

Table 6 The first two natural frequencies for the two crack geometries of beams at 745 mm from the cantilevered end.

Natural frequencies	***Crack depth***						
Hz	***Intact beam***	***5 mm***	***10 mm***	***15 mm***	***20 mm***	***25 mm***	***30 mm***
f_1(FEM V-shaped)	15.993	15.982	15.941	15.866	15.734	15.487	15.035
f_1(FEM new crack)	15.993	15.981	15.938	15.859	15.72	15.463	14.954
f_2(FEM V-shaped)	98.757	98.258	96.451	93.448	88.781	81.673	72.413
f_2(FEM new crack)	98.757	98.194	96.324	93.146	88.326	81.06	71.098

The ANN model was trained using the dataset of V-shaped cracked cases only. The model was used to predict the crack locations and depths in beams with V-shaped cracks or a combination of rectangular and V-shaped cracks. Figure 10 and 11 clearly show that the ANN model gives a good prediction for the crack depths and locations. Table 7 and 8 show the predicted crack depths and locations for V-shaped and a combination of rectangular and V-shaped cracked cases. It is also found that, the ANN (Machine learning model) model gave good results for the crack depths and locations irrespective of the crack geometries, i.e., V-shaped and combination of rectangular and V-shaped cracked cases in beams.

From Figure 10 and 11, the machine learning model developed using the dataset of V-shaped cracked cases can predict the crack parameters, i.e., crack depth and crack locations, in the new cracked (combination of rectangular and V-shaped) model with good accuracy. When comparing the findings of Tables 7 and 8, it is evident that the ANN model performed well in predicting the crack depths and positions in the new cracked model (combination of rectangular and V-shaped) cases.

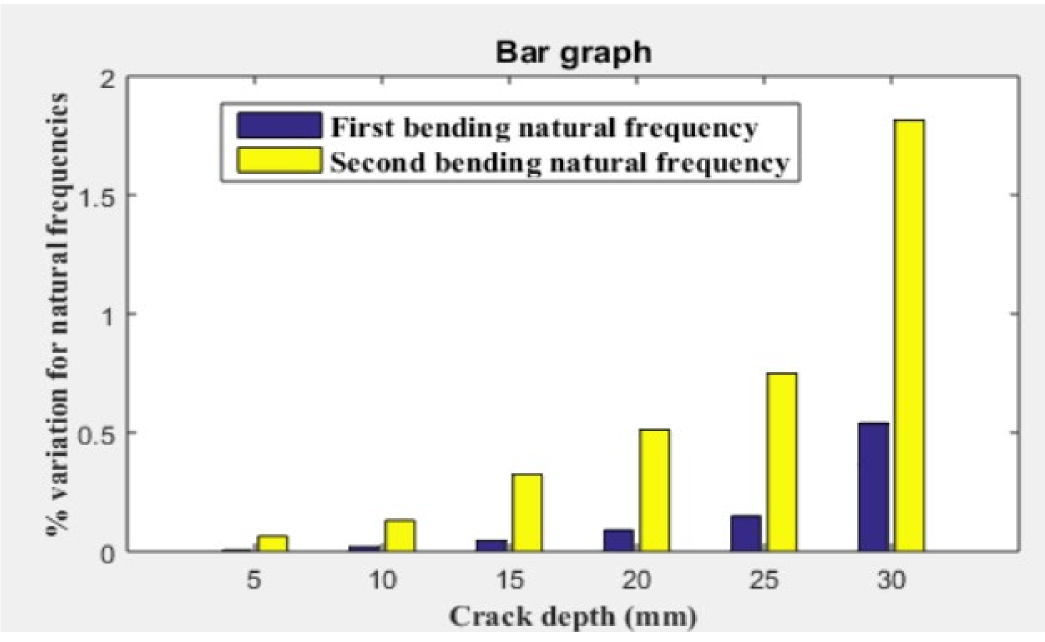

Figure 9. Percentage variation for natural frequencies between V-shaped and combination of rectangular and v-shaped crack

Table 7 Comparison between Actual and predicted ANN outputs of V-shaped cracked cases.

Sr. No.	f_{r1}	f_{r2}	f_{r3}	*a/H*	*a/H*	*% error*	L_1/L	L_1/L	*% error*
				Actual	*ANN*		*Actual*	*ANN*	
01	0.886325	0.970027	0.997558	0.4	0.3979	**0.525**	0.1115	0.1115	**0**
02	0.872007	0.966731	0.997262	0.422222	0.4208	**0.33684**	0.1115	0.1115	**0**
03	0.900206	0.990725	0.922543	0.466667	0.4619	**1.0214**	0.2654	0.2386	**10.0928**
04	0.888951	0.989702	0.914866	0.488889	0.4808	**1.6545**	0.2654	0.3539	**-33.353**
05	0.925968	0.880302	0.961410	0.533333	0.5345	**-0.2187**	0.4192	0.4266	**-1.7578**
06	0.916651	0.868819	0.958007	0.555556	0.5573	**-0.314**	0.4192	0.4234	**-0.9945**
07	0.958857	0.792060	0.936690	0.6	0.6044	**-0.7333**	0.5731	0.5752	**-0.3704**
08	0.953667	0.773819	0.934364	0.622222	0.6259	**-0.5910**	0.5731	0.5615	**2.0201**
09	0.988901	0.843272	0.778045	0.644444	0.6396	**0.7517**	0.7269	0.7269	**0.00317**
10	0.987369	0.825683	0.771311	0.666667	0.6494	**2.59**	0.7269	0.7269	**0.00317**

Table 8 Comparison between Actual and predicted ANN outputs of new crack model (combination of rectangular and V-shaped)

Sr. No.	f_{r1}	f_{r2}	f_{r3}	*a/H*	*a/H*	*% error*	L_1/L	L_1/L	*% error*
				Actual	*ANN*		*Actual*	*ANN*	
01	0.8863224	0.9700274	0.9975510	0.4	0.3988	**0.3**	0.1115	0.1138	**-2.0275**
02	0.8720010	0.9667310	0.9972610	0.422222	0.4223	**-0.0184**	0.1115	0.1138	**-2.0275**
03	0.9002016	0.9907220	0.9225400	0.466667	0.4751	**-1.8071**	0.2654	0.2374	**10.544**
04	0.8889410	0.9897003	0.9148601	0.488889	0.4967	**-1.5977**	0.2654	0.3511	**-32.298**
05	0.9259616	0.8803015	0.9614028	0.533333	0.5196	**2.575**	0.4192	0.4518	**-7.7688**
06	0.9166414	0.8688120	0.9580036	0.555556	0.5442	**2.044**	0.4192	0.4471	**-6.6477**
07	0.9588510	0.7920580	0.9366822	0.6	0.6129	**-2.15**	0.5731	0.5701	**0.5194**
08	0.9536582	0.7738186	0.9343612	0.622222	0.6345	**-1.973**	0.5731	0.5713	**0.31007**
09	0.9889000	0.8432718	0.7780433	0.644444	0.6418	**0.4103**	0.7269	0.7201	**0.9386**
10	0.9873622	0.8256810	0.7713104	0.666667	0.6543	**1.855**	0.7269	0.7174	**1.3100**

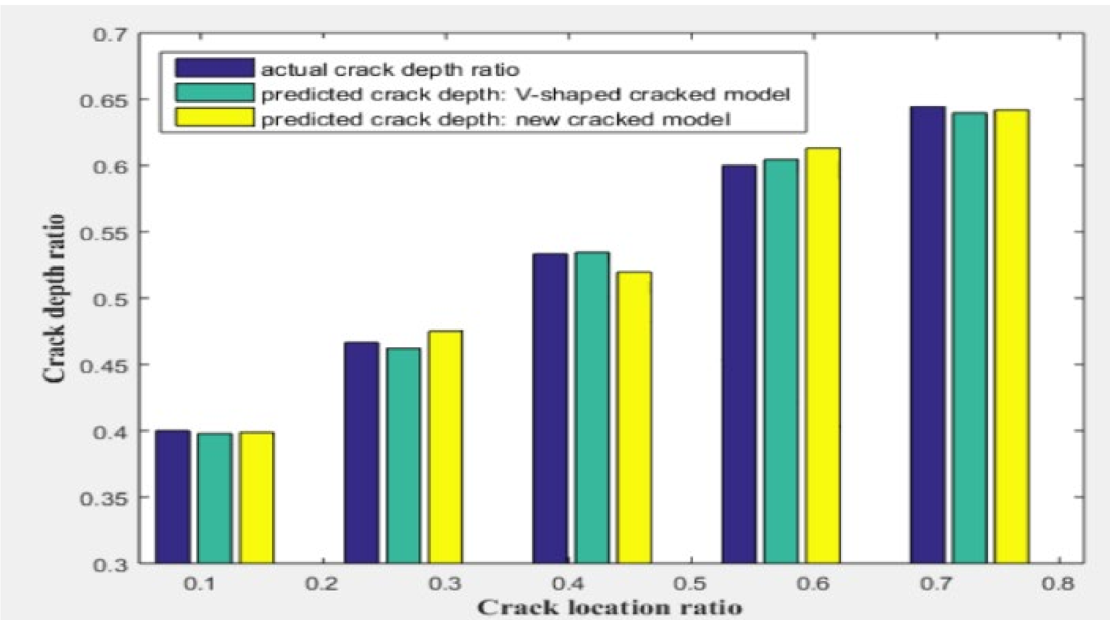

Figure 10. Predicted crack depth ratio at different crack locations using the machine learning model

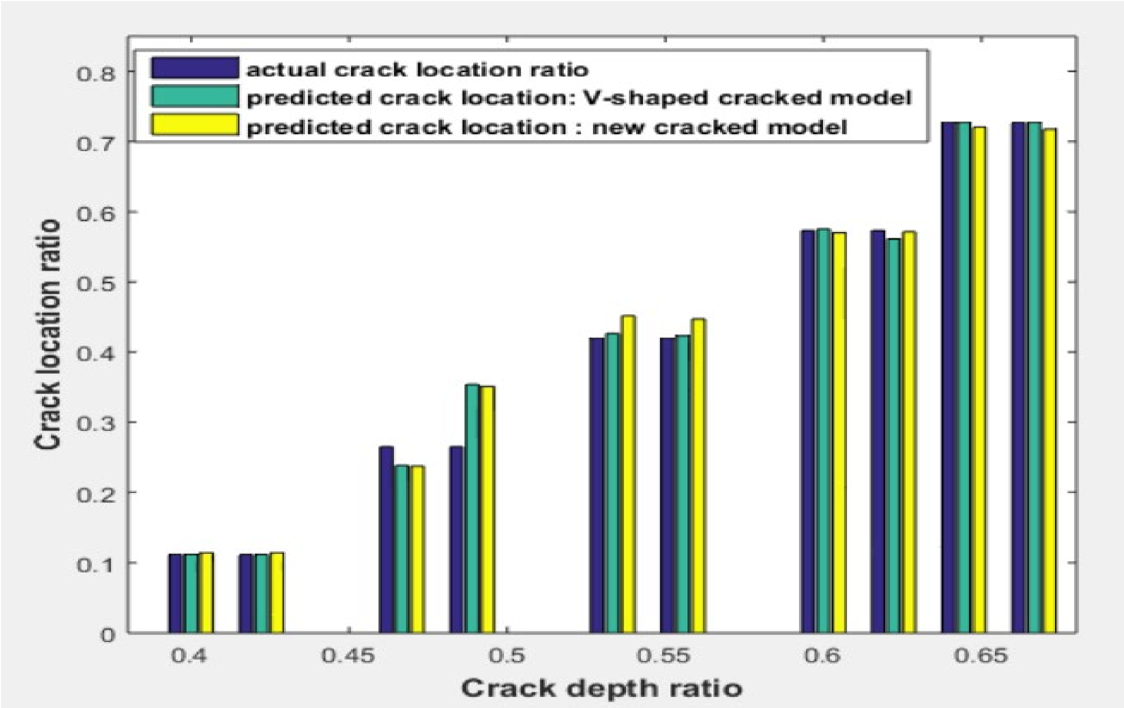

Figure 11. Predicted crack location ratio at different crack depths using the machine learning model

From this here we can conclude that ANN (Machine learning model) gives the better model for the crack depths and locations irrespective of the crack geometries, i.e., V-shaped and combination of rectangular and V-shaped cracked cases in beams.
It is also apparent that, for the identical configurations, the natural frequency decrease of new cracked model cases compared to an un-cracked beam is considerably larger than that of a V-shaped cracked beam. As a result, it is clear that as the difference in natural frequency between the un-cracked and cracked beams grows, the ANN model can more accurately predict the crack characteristics.

7 CONCLUSIONS

First, it has been observed that the natural frequencies drop as the composite beams' crack depth rises. A maximum difference of 1.815 percent was found when comparing the finite element natural frequency findings from the new and V-shaped crack models for the same configurations. The ANN model based on the data set of V-shaped cracked cases accurately predicted the crack location and depth in the cantilever beam irrespective of the crack geometry for the same configurations. Therefore, it is clear that the ANN model can predict the crack parameters, i.e., crack depth and locations, in the new cracked (combination of rectangular and V-shaped) model with reasonable accuracy. A neural controller can be programmed, trained, and installed in a structure, and this ANN controller will provide the damage information accurately.

REFERENCES

[1] Kisa. M. Free vibration analysis of a cantilever composite beam with multiple cracks, Composite Science and Technology, Vol. 64, 2004, 1391–1402.
[2] Krawczuk, M., Ostachowicz, W. and Zak, A. Modal analysis of cracked, unidirectional composite beam, Composites Part B: Engineering, Vol. 28, 1997, pp. 641–650.
[3] Song, O., Ha, T. W. and Librescu, L. Dynamics of anisotropic composite cantilevers weakened by multiple transverse open cracks, Engineering Fracture Mechanics, Vol. 70, 2003, pp. 105–123.
[4] Abd El-Hamid Hamada, A. An investigation into the eigennature of cracked composite beams, Composite Structures, Vol. 38, No. l–4, 1997, pp. 45–55.
[5] Wang, K. and Inman, D. J. Coupling of bending and torsion of a cracked composite beam, 22nd international modal analysis conference (IMAC), 26–29 January, Michigan, USA, 2004, pp. 1460–1472.
[6] W P P Aye and T M Htike, Inverse method for identification of crack using correlation model, SN Applied Sciences, 2019.
[7] S Orhan, L Murat, M H Dirikolu and G M Zorlu, The effect of crack geometry on non-destructive fault detection in a composite beam, International Journal of Acoustics and Vibration, Vol. 21, No. 3, 2016, pp. 271-273.
[8] Vakil-Baghmisheh, M.T., Peimani, M., Sadeghi, M.H., Ettefagh, M.M., *Crack detection in beam-like structures using genetic algorithms,* Applied soft computing, Vo. 8, No. 2, 2008, pp. 1150–1160.
[9] Khatir, A., Tehami, M., Khatir, S., Wahab, M.A. 2016, *Multiple damage detection and localization in beam-like and complex structures using coordinate modal assurance criterion combined with firefly and genetic algorithms,* Journal of Vibroengineering, Vol. 18, No. 8, pp. 5063–5073.

[10] Sutar, M.K., Pattnaik, S., Rana, J. *Neural Based Controller for Smart Detection of Crack in Cracked Cantilever Beam,* Materials Today: Proceedings, Vol. 2, No. 4-5, 2015, pp. 2648–2653.
[11] Nasiri, S., Khosravani, M.R., Weinberg, K., *Fracture mechanics and mechanical fault detection by artificial intelligence methods:* A review, Engineering Failure Analysis, Vol. 81, 2017, pp. 270–293.
[12] Teidj, S., Khamlichi, A., Driouach, A. 2016, *Identification of beam cracks by solution of an inverse problem,* Procedia Technology, Vol. 22, pp. 86–93.
[13] Thatoi, D.N., Choudhury, S., Das, H.C., Jena, P.K., Agrawal, G. 2014, CFBP Network–A Technique for Crack Detection, Procedia materials science, Vol. 6, pp. 10–17.
[14] Pan, D.G., Lei, S.S., Wu, S.C., *Two-stage damage detection method using the artificial neural networks and genetic algorithms,* International Conference on Information Computing and Applications, 2010, pp. 325–332.
[15] ANSYS Release 12.1, ANSYS Inc., (2010)
[16] Khalkar, V., and Ramachandran, S., The effect of crack geometry on non-destructive fault detection of EN 8 and EN 47 cracked cantilever beam. *Journal of Noise and Vibration Worldwide* Vol. 50, 2019, pp. 92–100.
[17] Khalkar, V., and Ramachandran, S., The effect of crack geometry on stiffness of spring steel cantilever beam. *Journal of low frequency noise, vibration and active control*, Vol. 37, 2018, pp. 762–774.
[18] Gillich, N., Tufisi, C., Sacarea, C., Rusu, C.V., Gillich, G., Praisach, Z., & Ardeljan, M., *Beam Damage Assessment Using Natural Frequency Shift and Machine Learning,* Sensors, Vol. 22, 2022, pp. 2–23.
[19] Tufisi, C., Gillich, N., Ardeljan, M., Paun, R.L., Rusu, V., & Gillich, G., *A Cost Function to Assess Cracks in Simply Supported Beams with Artificial Intelligence,* Romanian Journal of Acoustics and Vibration, Vol. 18, No. 1, 2021, pp. 46–52.
[20] Tufisi, C., Rusu, C.V., Gillich, N., Pop, M.V., Hamat, C.O., Sacarea, C., & Gillich, N. (2022). *Determining the Severity of Open and Closed Cracks Using the Strain Energy Loss and the Hill-Climbing Method,* Applied Science, Vol. 12, 2022, pp. 2–18.
[21] Tufisi, C., Rusu, V., & Gillich, G., *Locating Transverse Cracks in Prismatic Beams Using Random Forest Method and the Frequency Drop,* Romanian Journal of Acoustics and Vibration, Vol. 18, No. 2, 2021, pp. 119–125.
[22] Onchis, D.M., & Gillich, G., *Stable and explainable deep learning damage prediction for prismatic cantilever steel beam,* Computers in Industry, Vol. 125, 2021, pp. 1–8.

.